Journal of Power Sources 244 (2013) 482–487

Contents lists available at SciVerse ScienceDirect

Journal of Power Sources

journal homepage: www.elsevier.com/locate/jpowsour

$Li_4Ti_5O_{12}$ thin-film electrodes by sol–gel for lithium-ion microbatteries

J. Mosa [a], J.F. Vélez [a], J.J. Reinosa [a], M. Aparicio [a,*], A. Yamaguchi [b], K. Tadanaga [b], M. Tatsumisago [b]

[a] Instituto de Cerámica y Vidrio (CSIC), C/Kelsen 5, 28049 Madrid, Spain
[b] Department of Applied Chemistry, Graduate School of Engineering, Osaka Prefecture University, Sakai, Osaka 599-8531, Japan

HIGHLIGHTS

- Homogeneous, transparent and cracked-free Spinel $Li_4Ti_5O_{12}$ coatings.
- Influence of thermal treatment on the phase composition and electrochemical behavior.
- Deep structural characterization, including XRD, RBS, XPS and TOF-SIMS.

ARTICLE INFO

Article history:
Received 19 September 2012
Received in revised form
8 November 2012
Accepted 14 November 2012
Available online 23 November 2012

Keywords:
Li-ion microbatteries
Sol–gel
$Li_4Ti_5O_{12}$
Nanocrystalline materials
Thin film
Coatings

ABSTRACT

Spinel $Li_4Ti_5O_{12}$ has been considered as one of the most prospective anode materials for Li-ion microbatteries. Homogeneous, transparent and crack-free $Li_4Ti_5O_{12}$ coatings with thickness around 110 nm have been prepared by dipping gold-coated quartz substrates in sols prepared using titanium isopropoxide and lithium acetate. The influence of the thermal treatment on the phase composition, structure and electrochemical behavior was studied. Rutile TiO_2 (considered as an impurity in this study) is only detected in the coatings treated at 700 °C. XPS and TOF-SIMS depth profiles show a homogeneous distribution, with a Li increase and Ti reduction at the surface. Electrochemical characterization of samples treated at 600 °C presents a redox reaction around 1.55 V indicating that the film is simple phase of $Li_4Ti_5O_{12}$. The shift to slightly lower voltage in samples treated at 700 °C is a consequence of Rutile impurities. Larger capacity and good reversibility in the sample heat-treated at 600 °C can be attributed to high crystallinity of $Li_4Ti_5O_{12}$ and phase purity. RBS analysis specifies a composition close to $Li_4Ti_5O_{12}$ in the case of the pristine and charged samples, and $Li_7Ti_5O_{12}$ for the discharged sample. Surface XPS study confirms the presence of an outermost layer containing LiF and Li_2CO_3.

1. Introduction

Rechargeable lithium batteries have been utilized as efficient energy storage devices in many lightweight electronic appliances, cellular phones and laptop computers, because of the high energy densities. There have been many efforts to make microscale lithium batteries for various application fields related to microsystems, such as microsensors, micromechanics, and microelectronics [1–5]. The general requirements of the microbatteries for these applications are high specific energy, wide range of temperature stability, low self discharge rate and flexibility of cell design [6]. Thin film Li-ion batteries fabricated using only solid-state materials by a thin-film process are very beneficial because of its excellent safety and good rechargeability and are expected to fulfill the requirements above [7].

Among the different electrodes used, spinel $Li_4Ti_5O_{12}$ has been considered as one of the most prospective anode materials for Li-ion batteries because of its excellent reversibility and long cycle life. It has an excellent Li ion mobility and exhibits almost no structural change (zero-strain insertion material) during charge–discharge cycling [8–11]. Li-ion intercalation in $Li_4Ti_5O_{12}$ occurs via a two-phase coexistence process, resulting in a very stable (dis)charge voltage at around 1.55 V (vs. Li/Li^+). During the (dis) charging process the lithium content can be varied for $Li_xTi_5O_{12}$ between $4 < x < 7$, resulting in a maximum theoretical gravimetric capacity of 175 mAh g^{-1}. The lattice parameter for a spinel unit cell $(Li[Li_{1/3}Ti_{5/3}]O_4)_8$ is 8.36 Å [6,12].

* Corresponding author. Tel.: +34 917355840; fax: +34 917355843.
E-mail address: maparicio@icv.csic.es (M. Aparicio).

0378-7753/$ – see front matter © 2012 Elsevier B.V. All rights reserved.
http://dx.doi.org/10.1016/j.jpowsour.2012.11.037

Sol–gel route synthesis is a general and effective method for the preparation of micro/nanostructured materials with well controlled morphology and structure. However, the synthesis of spinel $Li_4Ti_5O_{12}$ using the sol–gel method has been mainly focused on the preparation of particles with optimized properties to improve electrochemical performance as particle size, doping with other elements, porosity, etc. In this case, a titanium alkoxide is usually used in combination with the following lithium salts: lithium carbonate [13], lithium acetate [14–16] or lithium nitrate [17]. Only a few recent publications have been devoted to the direct preparation of $Li_4Ti_5O_{12}$ coatings using the sol–gel method, and the aim now is to increase the knowledge of the material as a layer with the idea of assembling the necessary properties of stability, ionic conductivity and electrical conductivity to be used in a planar all-solid-state Li-ion microbatteries. In these devices, the electrolyte is also a solid layer and the complete cell can be manufactured using standard coating and film techniques [18–21].

Our previous work in this area studied mainly the influence of the Li/Ti molar ratio on the phase composition and structure to obtain almost pure spinel $Li_4Ti_5O_{12}$ thin films by dipping [22]. An excess of lithium precursor (Li/Ti = 6/5) with respect to the nominal composition was necessary to obtain the desired objective. Here, the objective is to study the influence of the thermal treatment of coatings (different temperatures and times) on the crystalline structure, homogeneity across the thickness and electrochemical behavior. We also report a detailed structural analysis of material and a thorough electrochemical characterization.

2. Experimental

The solution (atomic ratio Li/Ti = 6/5) was prepared using titanium isopropoxide (ABCR, 97%) and lithium acetate (Aldrich, 99.99%) as precursors, absolute ethanol (Panreac), acetic acid (Merck, 100%), water and HCl. Final molar ratios of Li:Ti:ethanol:-acetic acid:water:HCl were 6:5:120:10:13:0.1. Lithium acetate was first dissolved in alcohol and acetic acid, and subsequently titanium alkoxide, water and HCl were incorporated for starting the sol–gel hydrolysis and condensation reactions by stirring at room temperature for 2 h [22].

Viscosity (Sine-wave Vibro Viscometer SV-1A) and pH measurements of the sol were performed at room temperature. Quartz substrates were used to assess the homogeneity of the coating and thickness measurement; silicon substrates for X-ray measurements and gold coated (50 nm) quartz substrates, prepared by sputtering, for electrochemical characterization. One-layer coatings were prepared by dipping on different substrates using a withdrawal rate around 14 cm min^{-1}. Thermal treatments were carried out at 500, 600 and 700 °C and two treatment times, one and four hours.

Spectral Ellipsometric measurements were performed using a Variable Angle Spectroscopic Ellipsometer (WVASE32, M-2000UTM, J.A. Co., Woollam) to characterize thickness (e) and refractive index (n) of films deposited on quartz substrates. The spectra were taken in the visible region, between 250 and 900 nm at a variable incident angle of 65, 70 and 75°. The data were fitted using the WVASE32 software and taking into account a Cauchy model. Characterization of the coatings also includes analysis of a cross-section of coated samples performed by scanning electron microscopy (HITACHI S-4700 field emission). The crystal structure of coatings was characterized by Grazing incidence X-ray diffraction (step: 0.040° and angle: 0.5°) using a Siemens D-5000.

X-ray photoelectron spectroscopy (XPS) spectra were acquired on a K-Alpha – Thermo Scientific spectrometer with monochromatic Al Kα X-ray source (1486.68 eV). Compositional depth profiling of the coatings was obtained to evaluate the homogeneity of elements distribution through the coating. Surface chemical states of discharged and charged coatings on gold-coated quartz samples treated at 700 °C for 4 h were also studied by XPS using an Ar^+ ion source. Elements quantification was performed using the Shirley method for complete spectra and a peak fit program (Advantage 4.6 Thermo) for Li 1s.

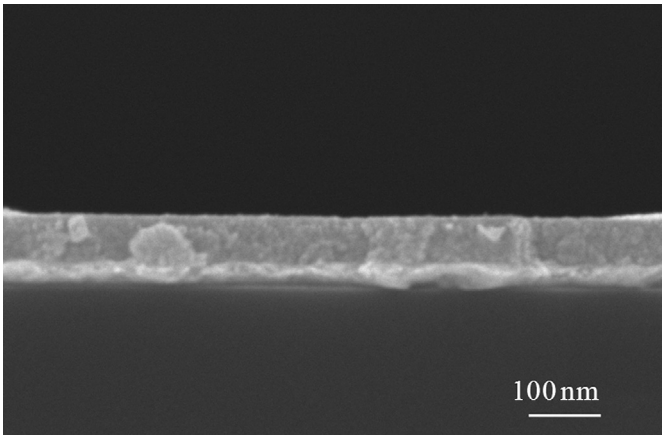

Fig. 1. Cross-section SEM micrograph of a coated sample treated at 600 °C for 4 h.

Compositional depth profiling of the three different samples: pristine, discharged and charged was also obtained using a TOF-SIMS 5 spectrometer (IonTof). A pulsed 25 keV Bi^+ primary ion source was employed for analysis, delivering 1.2 pA of target current over a 20.8 μm × 20.8 μm area. Sputtering was done using a 1 keV Oxygen beam over a 250 μm × 250 μm area. Data acquisition and post-processing analyses were performed using the IonSpec software.

The composition of the films (pristine, discharged and charged) was also analyzed by Rutherford Backscattering Spectrometry (RBS) using H^+ ions produced by the van de Graff accelerator of the Centro de Micro-Análisis de Materiales (CMAM), Madrid. $^7Li(\alpha,\alpha_0)^7Li$ resonance at 2050 keV was used to measure accurately the Li concentration. The incident ion beam with a diameter of 1 mm was normal to the specimen surface with 10 μC doze scattered ions detected by a mobile detector at 165°. Data were interpreted using the SIMNRA program.

Electrochemical behavior of the thin films prepared on Au/Quartz substrate was examined by a three electrode beaker cell using Li as the counter and reference electrodes, and 1 M $LiPF_6$/(EC–DEC) as liquid electrolyte.

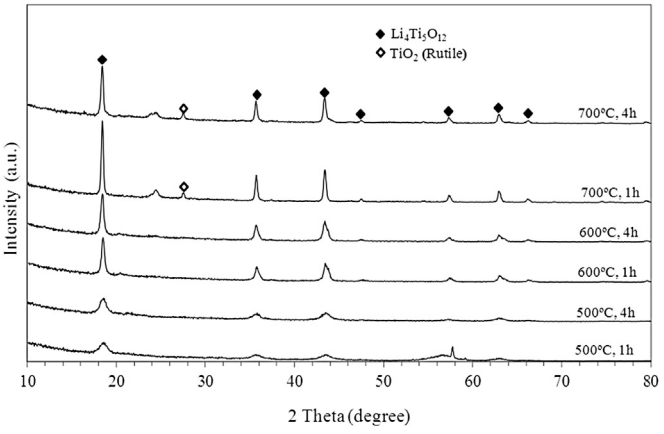

Fig. 2. Grazing incidence X-ray of coatings treated at 500, 600 and 700 °C for 1 and 4 h.

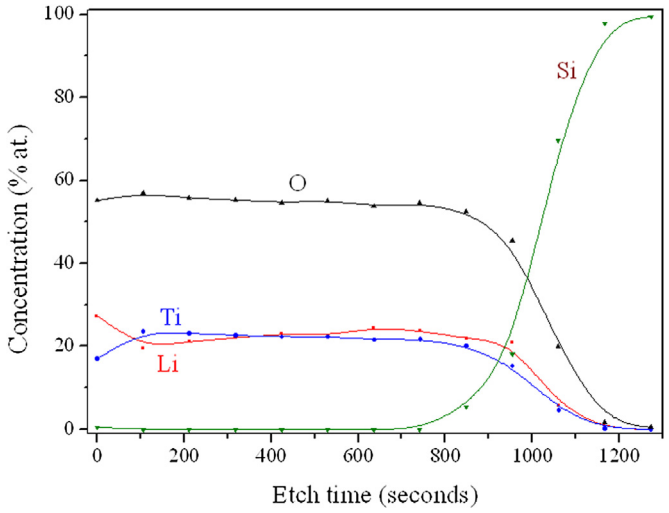

Fig. 3. XPS depth profiles of the coating on quartz treated at 600 °C for 1 h.

3. Results and discussion

The sol is transparent without the presence of phase separation or precipitates with a pH of 6.3 and viscosity values, just after the sol synthesis, between 2.5 and 2.8 mPa s for a temperature range of 26–24 °C. Viscosity measurements in the following days showed similar values, evidencing the absence of an accelerated aging of the sol.

Homogeneous and transparent coatings were prepared on the three substrates. Spectral ellipsometry measurements indicate a decreasing thickness with the increase of temperature and treatment time. The maximum thickness, 120 nm, was obtained after the thermal treatment at 500 °C for 1 h. On the other hand, the lower thickness (95 nm) was achieved with the heat treatment of 700 °C for 4 h. The cross-section SEM micrograph of a coated sample treated at 600 °C for 4 h (Fig. 1) presents a dense, homogeneous and well-bonded layer. The thickness of the coating is around 100 nm, in accordance with ellipsometry results.

Fig. 2 shows the grazing incidence X-ray results of coatings treated at 500, 600 and 700 °C for one and four hours. All the treatments present the face-centered cubic spinel $Li_4Ti_5O_{12}$ (JCPDS # 49-0207), although with greater intensity peaks with increasing the heat treatment temperature. Only the coatings treated at 700 °C for one and four hours show the presence of a second phase, Rutile TiO_2 (JCPDS # 21-1276).

XPS depth profiles of the coating on quartz treated at 600 °C for 1 h (Fig. 3) show a homogeneous distribution of Si, O, Ti y Li, which implies that experimental procedure (synthesis and thermal treatment of coatings) has been accurately performed. It can be observed an increase of lithium content together with a reduction of titanium concentration at the surface. This behavior can be associated with usual lithium diffusion, enhanced by the lithium excess used in the synthesis of the sol. Considering the values of

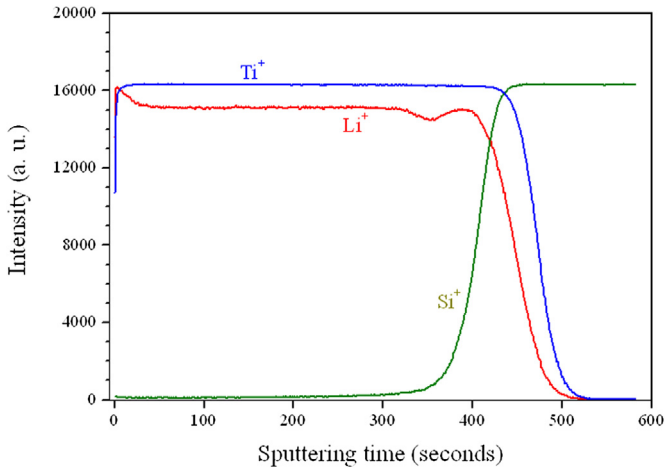

Fig. 4. TOF-SIMS depth profiles of the coating on quartz treated at 600 °C for 1 h.

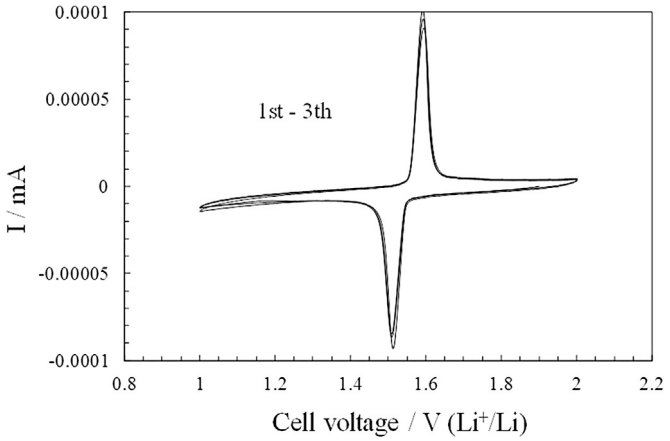

Fig. 5. Cyclic voltammogram (3 mV min^{-1}) of the coating treated at 600 °C for 4 h.

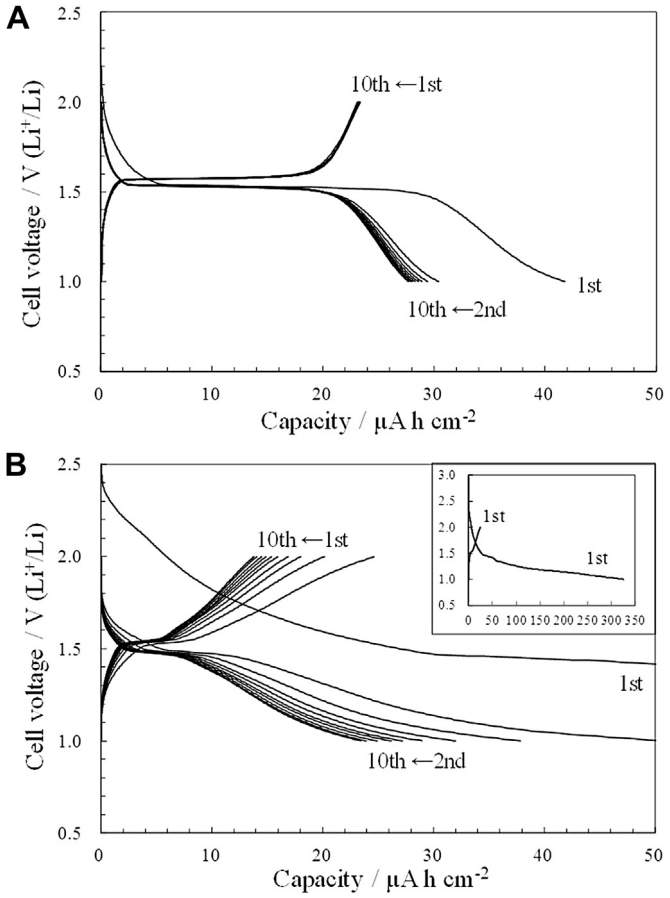

Fig. 6. Charge–discharge curves of coatings treated at 600 °C for 4 h (A) and 700 °C for 4 h (B).

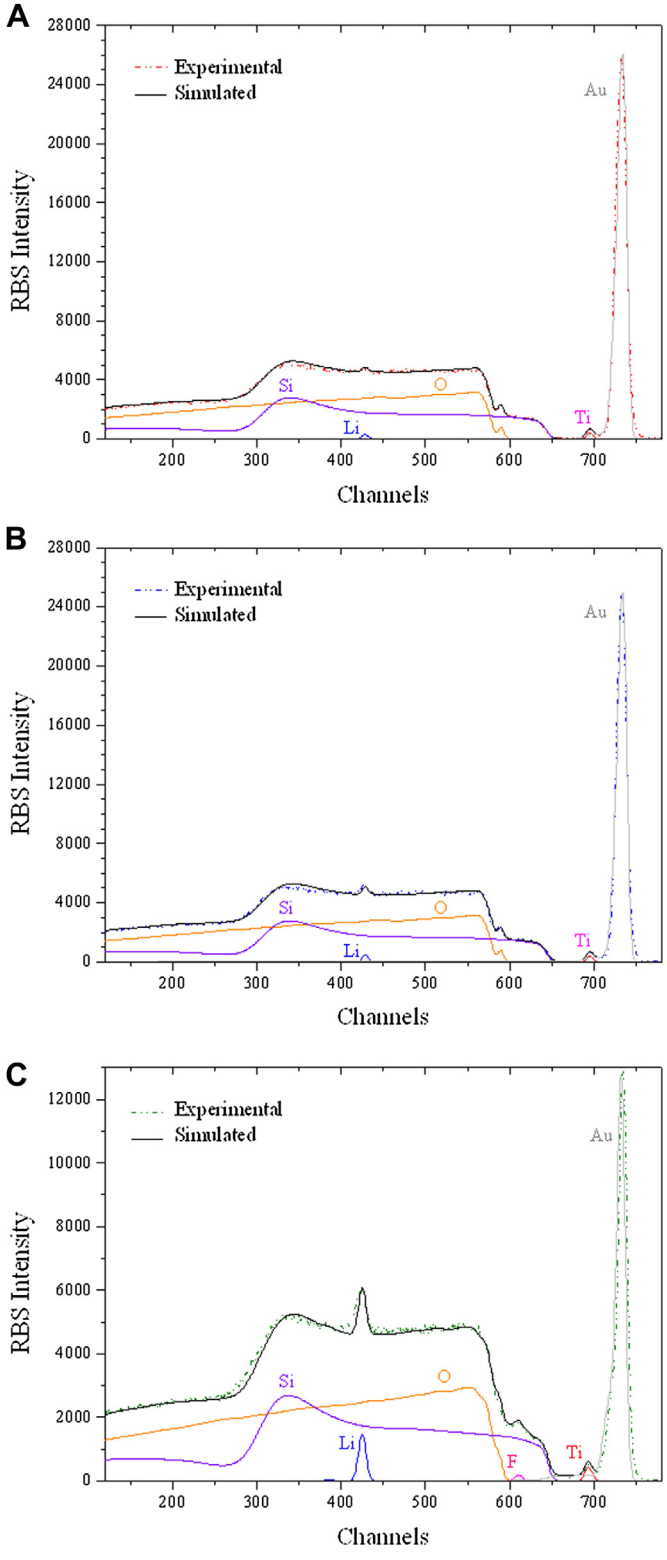

Fig. 7. RBS spectrum and simulation for the pristine (A), charged (B) and discharged (C) coatings treated at 700 °C for 4 h. The black solid line corresponds to the complete simulation, while the colored solid lines to the partial elemental spectra simulations. (For interpretation of the references to color in this figure legend, the reader is referred to the web version of this article.)

atomic percentages in the bulk of the coating, a composition close to the theoretical ($Li_4Ti_5O_{12}$), except for the lithium excess from the preparation of the sol, is obtained. Fig. 4 shows the TOF-SIMS depth profiles of the same coating, where also a very homogeneous elements distribution and the interface between coating and quartz substrate can be observed. Again, it is possible to observe a higher Li and lower Ti concentrations at the surface, although a more meticulous analysis is necessary. RBS and XPS surface analysis of pristine, charged and discharged coatings are presented later.

The electrochemical properties of the films were evaluated with cyclic voltammogram (CV). As a typical result, CV of the thin film heat-treated at 600 °C for 4 h is presented in Fig. 5. One anodic and cathodic sharp peak is observed in the thin film, indicating that the film is simple phase of $Li_4Ti_5O_{12}$ which shows good reversible redox reactions. The pair of redox reaction peaks located between 1.5 and 1.6 V is characteristic of electrochemical lithium insertion/extraction of $Li_4Ti_5O_{12}$ [23]. Fig. 6 shows the charge–discharge curves of a cell using the $Li_4Ti_5O_{12}$ thin films prepared on Au/Quartz substrate and heat-treated at 600 °C for 4 h and 700 °C for 4 h, up to the 10th cycle. The current density employed in the present study was 0.05 mA cm^{-2}. The cell was discharged to 1.0 V, and then charged and discharged between 2.0 V and 1.0 V. In the charge/discharge processes, typical plateau at around 1.55 V (vs. Li^+/Li) was observed for the sample treated at 600 °C, which is in agreement with the potentials showed in the cyclic voltammogram. A slightly lower voltage (1.50 V (vs. Li^+/Li)) was obtained with samples treated at 700 °C because of the presence of rutile impurities. This result is a voltage profile characteristic of a mixed phase. Rather large irreversible capacity was observed at the first cycle for both samples heat-treated at 600 and 700 °C. The reason for the large irreversible

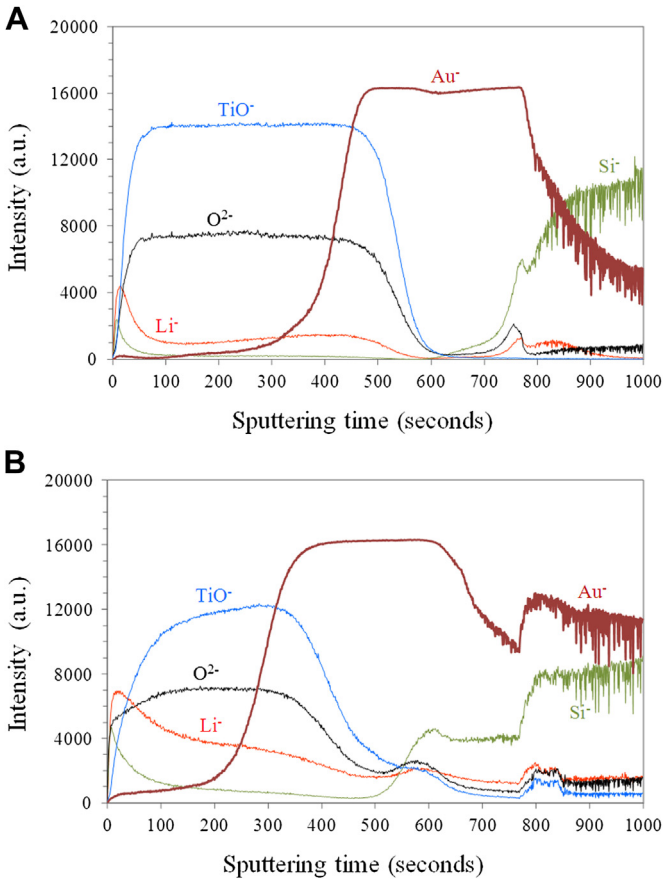

Fig. 8. TOF-SIMS depth profiles of the charged (A) and discharged (B) coatings treated at 700 °C for 4 h.

capacity is not clear, but may be due to the growth of a surface layer on the film surface [23]. In the thin film heat-treated at 600 °C for 4 h, the cell showed good cycling performance from 2 to 10 cycles. In contrast, the cell with thin film heat-treated at 700 °C shows a decrease in the discharge capacity during the charge/discharge cycling. The discharge capacity for the film heat-treated at 600 °C 4 h is larger than that of the film heat-treated at 700 °C 4 h. As shown in the XRD results, precipitation of TiO_2 was observed for the thin film heat-treated at 700 °C. Thus, larger capacity and good reversibility in the sample heat-treated at 600 °C can be attributed to high crystallinity of $Li_4Ti_5O_{12}$ and phase purity of the film.

Fig. 7 shows RBS spectrum and simulation (total and partial elemental spectra) for the pristine, charged and discharged coatings treated at 700 °C for 4 h. First, it was considered a single layer coating of lithium titanium oxide on the gold layer over the quartz substrate for the three samples. However, it was necessary to incorporate an outermost thin layer in the simulation to adjust properly the total spectrum. This thin layer in the pristine and charged samples mainly show Li and O with a small amount of Ti, while the discharged sample also presents a considerable amount of F due to the electrolyte diffusion during the electrochemical characterization. The second and main layer (lithium titanium oxide) has a composition close to $Li_4Ti_5O_{12}$ in the case of the pristine and charged samples. The discharged sample has an excess of lithium in this layer, as shown by the greater peak appearing around 425 value (*X* axis), which approximates to the theoretical composition of $Li_7Ti_5O_{12}$. Again, this second layer for the discharged sample shows a significant amount of F that can be explained by the residual porosity of the coating and the dragging effect of Li ions during insertion into the structure.

The presence of the outermost thin layer with a high Li and O contents was also previously observed in the XPS and TOF-SIMS depth profiles of pristine samples. TOF-SIMS depth profiles of the charged and discharged coatings treated at 700 °C for 4 h (Fig. 8)

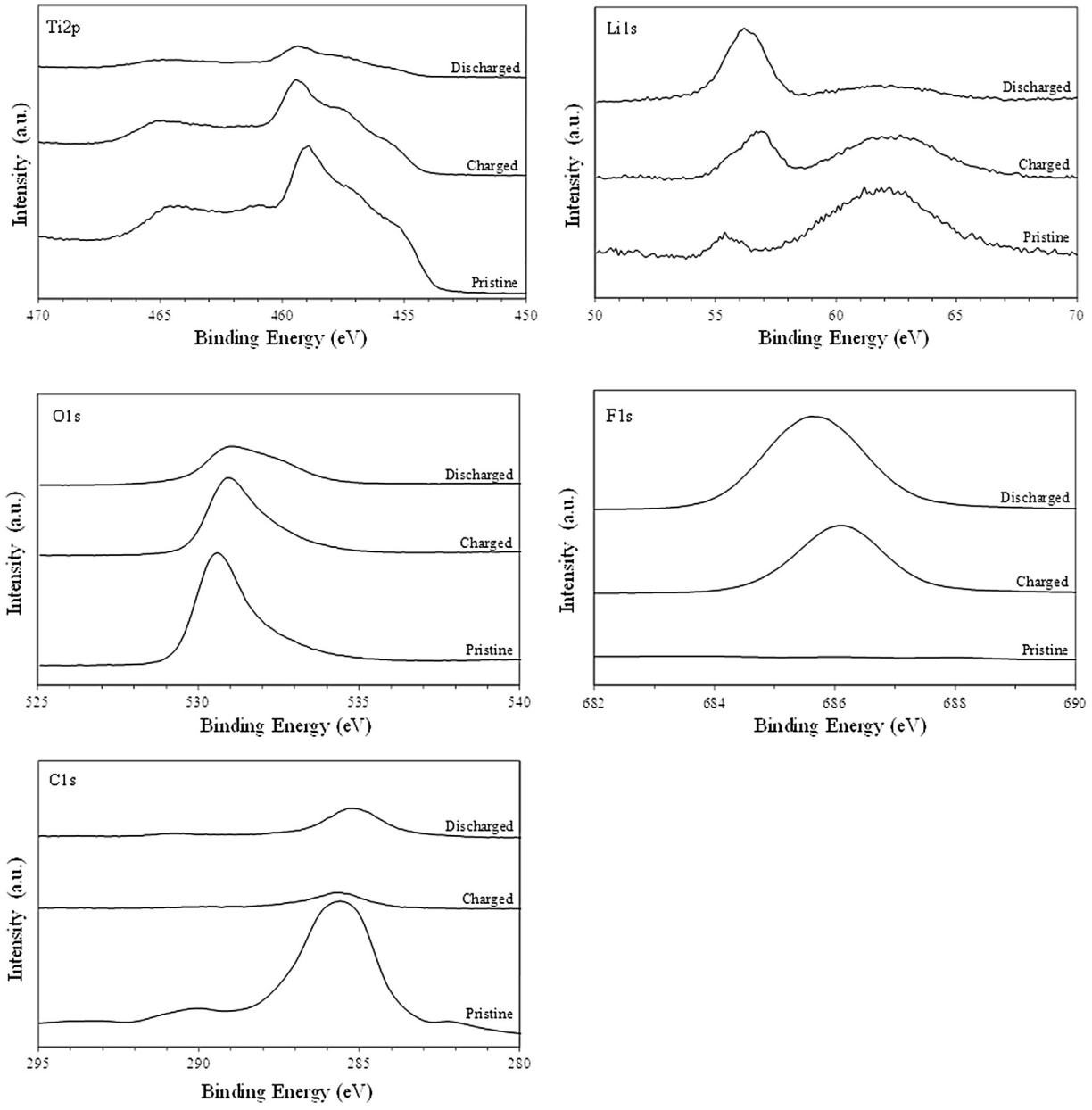

Fig. 9. XPS surface analysis of Ti2p, Li1s, O1s, F1s and C1s of pristine, charged and discharged coatings treated at 700 °C for 4 h.

also show a homogeneous distribution of elements, although somevariations can be observed as a consequence of the discharge–charge process. The location of the lithium titanium oxide layer/gold layer and gold layer/quartz substrate interfaces can be approximately determined by the intersection of the corresponding lines. A greater amount of lithium is evident in the discharged sample, in accordance with previously observed RBS results. Also, it is possible to observe the presence of the outermost thin layer with an increased Li concentration together with a Ti reduction.

However, in order to perform a more meticulous analysis of the surface composition, a surface XPS study of pristine, charged and discharged coatings treated at 700 °C for 4 h was performed (Fig. 9). The Ti2p signals indicate that pristine and charged curves are similar to each other compared with the discharged curve. This behavior is consistent with the fact that the pristine sample is initially charged. The signals present a $Ti2p_{3/2}$ peak centered at around 459.4 eV and a $Ti2p_{1/2}$ peak at 464.8 eV, near to those observed for TiO_2, indicating that the oxidation state of the Ti cations is mainly Ti(IV). The presence of a peak at 457.5 eV can be associated with the presence of the Ti(III) oxidation state. Although, this is only a surface analysis, it is possible to observe a lower Ti^{4+}/Ti^{3+} rate for the discharged sample, according to the insertion of lithium ions in the spinel structure [13,24]. Signals from Li1s, O1s, F1s and C1s indicate the presence of LiF and Li_2CO_3 in the outermost layer [25,26]. The amount of F is higher in the case of the discharged sample, and absent in the case of the pristine sample because the latter has not been in contact with the electrolyte. A higher amount of lithium carbonate is presented in the pristine sample as can be observed by the peaks in the O1s and C1s curves.

4. Conclusions

Cracked-free film-shaped spinel $Li_4Ti_5O_{12}$ electrodes with thickness around 110 nm were synthesized by sol–gel using titanium isopropoxide and lithium acetate. Rutile TiO_2 is only detected in the coatings treated at 700 °C using grazing incidence X-ray analysis. XPS and TOF-SIMS depth profiles of the coating show a homogeneous distribution of Si, O, Ti y Li, with an increase of lithium content together with a reduction of titanium concentration at the surface.

Electrochemical characterization of the coatings shows a couple of anodic and cathodic sharp peaks between 1.5 and 1.6 V (vs. Li^+/Li), characteristic of electrochemical lithium insertion/extraction of $Li_4Ti_5O_{12}$. Charge–discharge curves presents the typical plateau at around 1.55 V, although a rather large irreversible capacity was observed at the first cycle, may be due to the growth of a surface layer on the film surface. Larger capacity and good reversibility in the sample heat-treated at 600 °C can be attributed to high crystallinity of $Li_4Ti_5O_{12}$ and phase purity of the film.

It was necessary to incorporate an outermost thin layer in the RBS simulation to adjust properly the total spectrum. This thin layer mainly shows Li and O with a small amount of Ti, and a considerable amount of F due to the electrolyte diffusion. RBS analysis provides a composition close to $Li_4Ti_5O_{12}$ in the case of the pristine and charged samples, and $Li_7Ti_5O_{12}$ for the discharged sample. Surface XPS study confirms the presence of an outermost layer containing LiF and Li_2CO_3.

Acknowledgments

This work has been supported by the Spanish Science and Innovation Ministry under project PLE2009-0074 from National Program for I+D internationalising (ACI-PLAN E) and Japanese Science and Technology Agency (JST). J. Mosa acknowledges JAE-Doc program of CSIC and European Social Found (ESF) for financial support. The authors wish to thank Miguel Gómez, Alicia Durán, Pedro Luque and David Martín y Marero for their help in the experimental procedure. The technical and human support provided by Daniel Gamarra (Facility of Analysis and Characterization of Solids and Surfaces of SAIUEx, financed by UEX, Junta de Extremadura, MICINN, FEDER and FSE) is recognized.

References

[1] K. Dokko, J. Sugaya, H. Nakano, T. Yasukawa, T. Matsue, K. Kanamura, Electrochem. Commun. 9 (2007) 857–862.
[2] M. Armand, J.M. Tarascon, Nature 451 (2008) 652–657.
[3] P.G. Bruce, B. Scrotasi, J.M. Tarascon, Angew. Chem. Int. Ed. 47 (2008) 2930–2946.
[4] J. Chen, F.Y. Cheng, Acc. Chem. Res. 42 (2009) 713–723.
[5] B. Peng, J. Chen, Coord. Chem. Res. 283 (2009) 2805–2813.
[6] J.F.M. Oudenhoven, L. Baggetto, P.H.L. Notten, Adv. Energy Mater. 1 (2011) 10–33.
[7] Y.J. Park, K.S. Ryu, Y.S. Hong, S.H. Chang, J. Electrochem. Soc. 149 (2002) 597–602.
[8] L. Cheng, H.J. Liu, J.J. Zhang, H.M. Xiong, Y.Y. Xia, J. Electrochem. Soc. 153 (2006) A1472–A1477.
[9] K. Ariyoshi, S. Yamamoto, T. Ohzuku, J. Power Sources 119–121 (2003) 959–963.
[10] T. Ohzuku, A. Ueda, N. Yamamoto, J. Electrochem. Soc. 142 (1995) 1431–1435.
[11] A.D. Pasquier, A. Laforgue, P. Simon, J. Power Sources 125 (2004) 95–102.
[12] Y. Bai, F. Wang, F. Wu, C. Wu, L. Bao, Electrochim. Acta 54 (2008) 322–327.
[13] Y. Hao, Q. Lai, D. Liu, Z. Xu, X. Ji, Mater. Chem. Phys. 94 (2005) 382–387.
[14] B. Zhang, Z.D. Huang, S.W. Oh, J.K. Kim, J. Power Sources 196 (2011) 10692–10697.
[15] H. Xiang, B. Tian, P. Lian, Z. Li, H. Wang, J. Alloy. Compd. 509 (2011) 7205–7209.
[16] C. Jiang, Y. Zhou, I. Honma, T. Kudo, H. Zhou, J. Power Sources 166 (2007) 514–518.
[17] M.R. Mohammadi, D.J. Fray, J. Sol-Gel Sci. Technol. 55 (2010) 19–35.
[18] J. Haetge, P. Hartmann, K. Brezesinski, J. Janek, T. Brezesinski, Chem. Mater. 23 (2011) 4384–4393.
[19] L. Shen, C. Yuan, H. Luo, X. Zhang, K. Xua, F. Zhang, J. Mater. Chem. 21 (2011) 761–767.
[20] Y.H. Rho, K. Kanamura, J. Electrochem. Soc. 151 (2004) A106–A110.
[21] L. Kavan, M. Grätzel, Electrochem. Solid State Lett. 5 (2002) A39–A42.
[22] J. Mosa, J.F. Vélez, I. Lorite, N. Arconada, M. Aparicio, J. Power Sources 205 (2012) 491–494.
[23] J. Li, Y.L. Jin, X.G. Zhang, H. Yang, Solid State Ion. 178 (2007) 1590–1594.
[24] M.C. Biesinger, L.W.M. Lau, A.R. Gerson, R.S.C. Smart, Appl. Surf. Sci. 257 (2010) 887–898.
[25] P. Verma, P. Maire, P. Novák, Electrochim. Acta 55 (2010) 6332–6341.
[26] J.T. Li, J. Swiatowska, V. Maurice, A. Seyeux, L. Huang, S.G. Sun, P. Marcus, J. Phys. Chem. C 115 (2011) 7012–7018.